Silicon Carbide - Graphene Nano-Gratings on 4H and 6H Semi-Insulating SiC

S. Mathew[1,a], S.P. Lebedev[2,b], A.A. Lebedev[2,c], B. Hähnlein[3,d],
J. Stauffenberg[4,e], E. Manske[4,f] and J. Pezoldt[1,g*]

[1]FG Nanotechnologie, Institute für Mikro- und Nanoelektronik and Institut für Mikro- und Nanotechnologien MacroNano®, PF 100565, 98684 Ilmenau, Germany

[2]Ioffe Physical Technical Institute, Russian Academy of Sciences, St. Petersburg, 194021 Russia

[3]FG Technische Physik I, Institut für Physik and Institut für Mikro- und Nanotechnologien MacroNano®, TU Ilmenau, Postfach 100565, 98684 Ilmenau, Germany

[4]FG Fertigungs- und Präzisionsmesstechnik, Institut für Prozessmess- und Sensortechnik and Institut für Mikro- und Nanotechnologien MacroNano®, PF 100565, 98684 Ilmenau, Germany

[a]sobin.mathew@tu-ilmenau.de, [b]lebedev.sergey@mail.ioffe.ru, [c]shura.lebe@mail.ioffe.ru, [d]bernd.haehnlein@tu-ilmenau.de, [e]jaqueline.stauffenberg@tu-ilmenau, [f]eberhard.manske@tu-ilmenau.de, [g]joerg.pezoldt@tu-ilmenau.de

Abstract. A technical methodology of fabrication of hierarchically scaled multitude graphene nano gratings with varying pitches ranging from the micrometer down to sub 40 nm scale is proposed. These are combined with sub 10 nm step heights on 4H and 6H semi-insulating SiC for length scale measurements is proposed. The nano gratings were fabricated using electron-beam lithography combined with dry etching of graphene, incorporating a standard semiconductor processing technology. A scientific evaluation of critical dimension, etching step heights, and surface characterization of graphene nano grating on both polytypes were compared and evaluated.

Introduction

SiC has attracted different perspectives of scientific applications owing to its predominant physical properties. In particular, the large bandgap, low intrinsic carrier concentration, high breakdown field strength, and numerous polytypes make SiC, a promising candidate for high performance applications and microelectromechanical systems [1,2]. However, for many applications, understanding and revealing the impact of substrate surface morphology and surface instabilities in SiC like nano-faceting, step bunching, and step meandering is crucial [3]. Understanding these nanoscale interface interactions requires a profound knowledge of the material at the atomic scale. It further demands the necessity of advanced characterization tools to generate new multidisciplinary knowledge about nanoscale phenomena. Consequently, an extensive improvement of available metrology methods and technologies for subatomic measurement for many ambitious research approaches at the atomic level is necessary.

Currently, laser interferometers are often used in high-resolution measurement applications. Based on the suitable laser scale today, a resolution of 5 pm can be achieved [4]. But these techniques confront many technological complexities due to the ever-increasing nonlinear problems in fringe interpolation [5]. However, the feasibility of using atomic lattices as the length scale standard was first demonstrated by Aketagawa on highly oriented pyrolytic graphite (HOPG) in 2007 [6] and paved a new basis for forthcoming research methods. Our aim is to apply this idea on epitaxial graphene to demonstrate atomic lattices with a perfect crystallographic structure for new subatomic measurement techniques. Using standard planar semiconductor processing technology, a hierarchically scaled multitude grating structure is developed and demonstrated, i.e., a diffraction grating consisting of different pitches with an atomic-scale resolution. Furthermore, these designed grating structures can be analysed with the nanofabrication machine (NFM-100). This machine is equipped with a tip-based

measuring system and has a positioning range of 100 mm in diameter with sub-nanometre precision [7]. However, it is crucial to make an appropriate material choice for this approach. Since this method is dependent on the lattice parameters of the material, a material that can withstand and make weak interaction with the environment in terms of oxidation is needed.

Considering the prerequisite properties of the material and feasibility of surface structuring with possible technologies, here we choose graphene grown on semi-insulating SiC for the study. We propose a design combining diffraction gratings consisting of different ridge widths and pitches ranging from the micro- to the sub-40 nm scale. Moreover, here we try to explore and investigate the possibility of understanding the surface morphology of graphene formed on 6H and 4H SiC polytypes and their inhomogeneity in interface roughness for length scale measurement purposes.

Experimental

Epitaxial graphene was grown on the Si-face of on-axis semi-insulating 4H-SiC and 6H-SiC. The graphitization process was carried out in a high-temperature furnace between 1800°C and 1900°C in an argon atmosphere at atmospheric pressure using the two-step methods [8-10]. For structuring and fabrication of graphene gratings, the samples were cleaned and spin-coated at 4000 rpm with a high-resolution negative resist, hydrogen-silsesquioxane (HSQ) (XR-1541-4%) and immediately baked on a hot plate at 90°C. The final resist thickness was about 30 nm. For high-resolution patterning and fabrication of nano gratings on graphene, we employed electron beam lithography at 20 kV and 7 μm aperture in a Raith 150 system [11]. Subsequently, the exposed structures were developed with a twostep process in a solution of 3:1 (DI: TMAH) and 9:1(DI: TMAH) for 1 min at room temperature. The samples were etched using an inductively coupled plasma etching technique with oxygen for 30 s. After etching, the resist was removed by buffered oxide etching (BOE) for 1 min and rinsed in DI for another 1 min. Evaluation and characterization of critical dimensions and etching step heights of the structured gratings were carried out using scanning electron microscopy (SEM) and atomic force microscopy (AFM) in non-contact mode. Here we employed AFM tips with a diameter below 20 nm.

Results and Discussion

The AFM images in Fig.1(a) and (b) illustrate the surface morphology and profile obtained from the pristine epitaxial graphene grown on the Si-face of semi-insulating 6H and 4H SiC polytypes. The
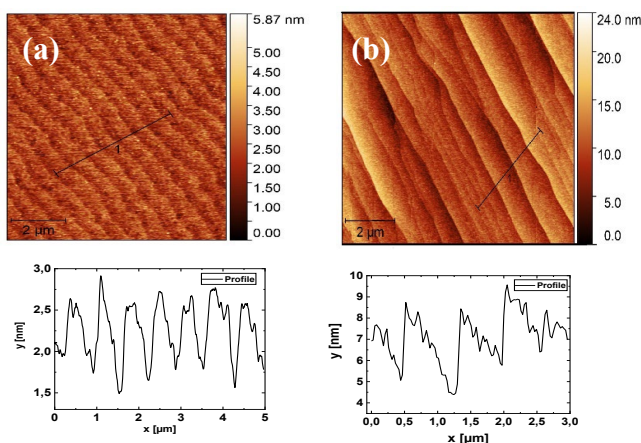

Fig. 1. Surface topography AFM images of bare graphene samples on (a) 6H and (b) 4H-SiC with their respective height profile.

graphene formed on the 6H-SiC surface is provided parallelly placed macro steps structures. During the graphitization process, these macro step like terraces are formed on the surface of SiC and distributed along the step edges of the SiC substrate due to the step bunching process [12]. Moreover, terraces formed on 6H-SiC periodically separated with step edges with an average width of 500 nm. The micro-steps formed on the step edges have an average height of 1.5 nm. Interestingly, the macro steps are evenly aligned, and their step edges are moderately straight. Furthermore, these step edges act as nucleation centres for graphene formation. As the Si and C edge atoms are weakly bonded, a variation of the graphene layer thickness in this region often occurs [13]. The average root mean square (RMS) roughness obtained from the graphene surface on the terrace is 0.9 nm. Besides the 6H-SiC, the

surface morphology of graphene formed on 4H-SiC was comparatively different with a combination of larger and smaller terraces. Fig 1 (b). shows the topography of graphene surface and its profile obtained from the scanned direction. The presence of wide and narrow terraces indicates the inhomogeneity in graphene layer thickness. According to the profile the formed terraces are from 1.5 μm to 2 μm wide. The height of the terrace steps varies between 3 and 6 nm.

The (RMS) roughness obtained from the graphene surface on the terrace is 0.6 nm. Furthermore, since these macro step like structures alter the homogeneity of the graphene surface, it is necessary to obtain samples with minimum surface instabilities for grating fabrication. Consequently, these imperfections must be considered during the fabrication of gratings. Fig 2. (a) and (b) shows AFM surface topology images of graphene line gratings obtained from both polytypes and their surface profiles. It is worth noting that the surface profile obtained from the line gratings on 6H-SiC shows a homogenous pattern. The
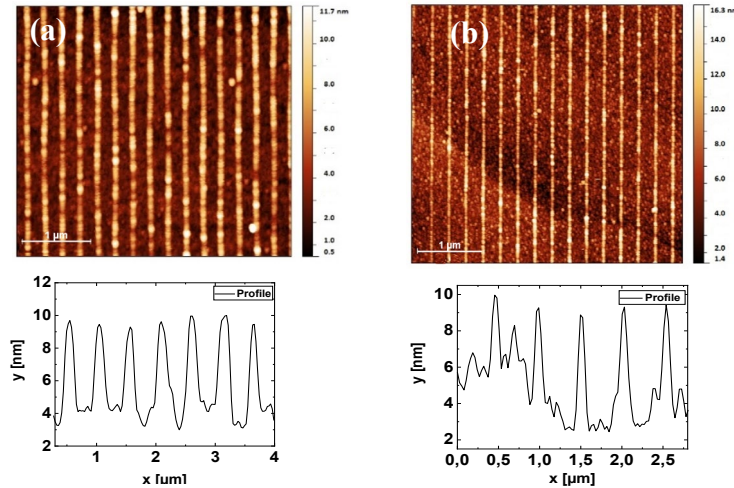
Fig. 2. AFM image of graphene line gratings and their surface profile obtained from both SiC polytypes (a) 250 nm pitch graphene line gratings on 6H-SiC and (b) Graphene line gratings with 250 nm pitch on 4H-SiC.

step heights and pitches obtained are comparably equal and uniform. And this behaviour is evident in all other structures with different pitch sizes of the graphene gratings obtained from 6H-SiC. Since the sample has homogenous morphology with evenly equal terraces and step-edges, the gratings formed on the 6H-SiC are similar. Apart from this, the graphene line gratings obtained from 4H-SiC show an inhomogeneity in step heights. This irregularity in the graphene grating structure is predominantly visible in the profile line scan obtained from the terrace region and caused by the underlying terrace edges.

Additionally, it further contributes to the distinct line width and causes instability and irregular construction of gratings and surface profile. The graphene grating line widths were obtained for a constant exposure dose of (600 pC/cm) with different pitches.
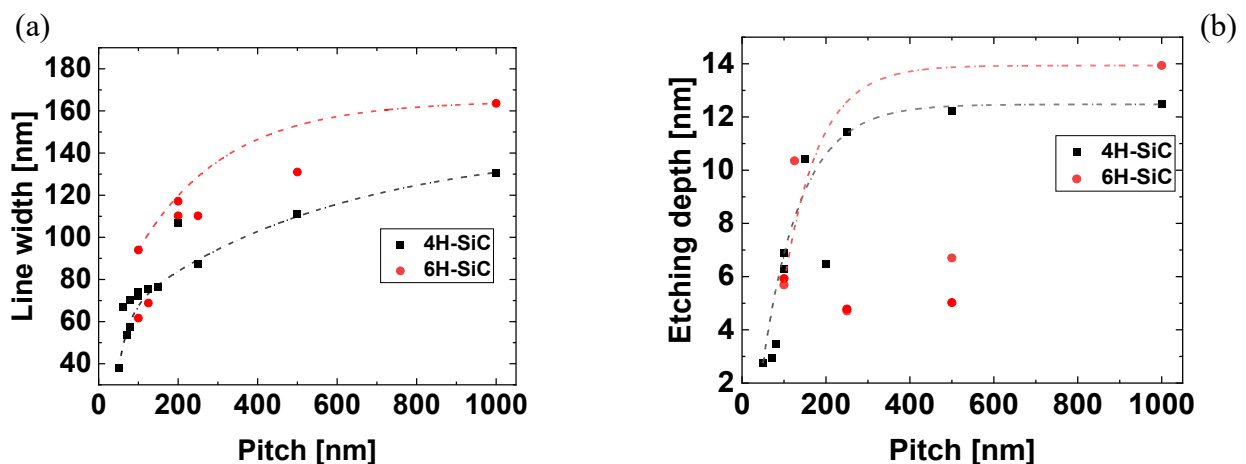

Fig. 3. (a) shows the dependency of the structured graphene line width of graphene gratings obtained after the etching process in semi-insulating 4H-SiC and 6H-SiC substrates, respectively and (b) dependency of the etching depth of graphene gratings

We estimated the critical dimension of the line gratings by analysing the grayscale intensity profile of the SEM image according to the methodology developed in [14]. The dependency of measured line widths of graphene gratings after etching is illustrated in Fig 3. (a). The line widths are increasing with pitch size independent of substrate polytype. The persistent charge accumulated in the semi-insulating SiC substrate might explain this unexpected behaviour. Furthermore, the substrate charging and persistent residual charges while examining the gratings on semi-insulating substrates also influence the line widths [11]. Moreover, the presence of large terraces of 4H SiC surfaces further alters the charging of the semi-insulating substrate. Therefore, backscattered electrons lead to a dose variation in the resist and consequently to a variation of the line width. The narrow linewidths obtained for lower pitches in 4H SiC further support the interpretation. Interestingly, the average line width for the same pitch on 6H-SiC is larger than the line widths on 4H-SiC, supporting the interpretation of the line width dependence on the persistent charge accumulated during the electron beam exposure due to the lower bandgap of 6H-SiC. However, we could also observe larger line widths for lower pitches in 6H-SiC, and this might be originating due to the intra and inter proximity effects during the electron beam exposure [15,16]. Importantly, the polytype structure, the polarity and the misorientation affects the step bunching [17]. Due to the higher repulsive force between steps on 6H surfaces compared to 4H the 6H surface is more stable against step height fluctuations and step bunching [17]. This might explain the observed formation of large terraces and large step heights in the 4H case. As a result the graphene gratings formed on both polytypes have distinct structural variations affecting the critical dimension.

We further evaluated the dependency of etch depth on the line density (pitch) of graphene line gratings obtained from both polytypes. Fig. 3(b) shows the etch depth obtained from the AFM measurements. The etching depths obtained from different gratings with varying pitches at constant exposure doses are additionally shown. The etching depths obtained from both 6H and 4H-SiC show a similar behaviour. Considering the etch depth profiles obtained from both samples, we could observe a contracting behaviour with decreasing pitch size. This decreasing pattern in the etching depth is due to the micro loading effect [18, 19], which reduces the etch rate along with diminishing opening dimension due to transport limitations. Furthermore, the average root mean square (RMS) roughness obtained from the grating surface of 4H-SiC is less (0.09 nm) than the RMS value (0.45 nm) obtained for 6H-SiC. However, in 6H-SiC, the surface waviness and roughness obtained from beneath the graphene gratings are minimized. The roughness along the graphene lines is comparable for both polytypes and has an average value of 0.06 nm.

Summary

A multitude of grating designs consisting of gratings with different pitches ranging from the micrometre down to sub 40 nm scale combined with sub 10 nm step heights on 4H and 6H semi-insulating SiC for length scale measurements has been demonstrated. The gratings obtained on 6H-SiC are preferable due to the absence of step bunching at the graphene formation conditions studied. So, the graphene formation conditions must be chosen in such a way that step bunching is suppressed.

Acknowledgements

References

[1]   H. Okumura, Jpn. J. Appl. Phys. 45 (2006) 7565.

[2]   M. Mehregany, C. A. Zorman, N. Rajan e.a., Proc. IEEE, 86, 8, (1998), 1594–1610.

[3]   Y. Tabuchi, K. Ashida, M. Sonoda, e.a., J. Appl. Phys. 122 (2017) 075702.

[4]   Laser interferometer Model SP 5000 NG. SIOS Meßtechnik GmbH. https://sios.de/wp-content/uploads/2020/05/SP-NG_TechnDaten_dt.pdf; last seen 12 February 2021.

[5]   T. Hausotte, B. Percle, U. Gerhardt e.a., Meas. Sci. Technol. 23 (2012) 074004.

[6]   M. Aketagawa, H, Honda, M. Ishige, C. Patamaporn, Meas. Sci. Technol. 18, (2007), 342-349.

[7]   J. Stauffenberg, I. Ortlepp, U. Blumröder, e.a., tm-Technisches Messen, (2021), 581-589.

[8]   I.A. Eliseyev, V.Yu Davydov, A.N. Smirnov e.a., Semiconductors 53 (2019) 1904-1909.

[9]   R. Göckeritz, D. Schmidt, M. Beleites e.a. Mater. Sci. Forum 679-680 (2011) 785-788.

[10] B. Hähnlein, S. P. Lebedev, I.A. Eliseyev e.a., Carbon 170 (2020) 666-676.

[11] B. Hähnlein, M. Breiter, T. Stauden, e.a., Mater. Sci. Forum 897 (2017) 735–738.

[12] J. Penuelas, A. Ouerghi, D. Lucot e.a., Phys. Rev. B 79 (2009) 033408.

[13] W. Norimatsu and M. Kusunoki, Physica E 42 (2010) 691.

[14] M. Hatzakis, Appl. Phys. Lett. 18 (1971) 7-10.

[15] T.H.P. Chang, J. Vac. Sci. Technol. 12 (1975) 1271-1275.

[16] M. Parikh, J. Appl. Phys. 50 (1979) 4371-4377.

[17] N. Ohtani, M. Katsuno, T. Aigo e.a. J. Cryst Growth 210 (2000) 613-622.

[18] J. Yeom, Y. Wu, J.C. Selby e.a., J. Vac. Sci. Technol. B 23 (2005) 2319-2329.

[19] K. Zekentes, J. Pezoldt and V. Veliadis, Mater. Res. Forum 69 (2020) 175-232.